Dependence of Corneal Epithelial Cell Proliferation on Modulation of Interactions Between ERK1/2 and NKCC1

Zheng Wang[1], Victor N. Bildin[1], Hua Yang[1], José E. Capó-Aponte[1,2], Yuanquan Yang[1] and Peter S. Reinach[1]

[1]Department of Biological Sciences, State University of New York, State College of Optometry, New York, NY, [2]Visual Sciences Branch, U.S. Army Aeromedical Research Laboratory, Fort Rucker, AL

Abstract

Epidermal growth factor (EGF) receptor stimulation or protein kinase C (PKC) activation enhances corneal epithelial cell proliferation. This response is needed to maintain corneal transparency and vision. We clarify here in human corneal epithelial cells (HCEC) the cause and effect relationships between ERK1/2 and NKCC1 phosphorylation induced by EGF receptor or PKC activation. Furthermore, the roles are evaluated of NF-κB and ERK1/2 in mediating negative feedback control of ERK1/2 and NKCC1 phosphorylation through modulating DUSP1 and DUSP6 expression levels. Intracellular Ca^{2+} rises induced by EGF elicited NKCC1 phosphorylation through ERK1/2 activation. Bumetanide suppressed EGF-induced NKCC1 phosphorylation, transient cell swelling and cell proliferation. This cause and effect relationship is similar to that induced by PKC stimulation. NKCC1 activation occurred through time-dependent increases in protein-protein interaction between ERK1/2 and NKCC1, which were proportional to EGF concentration. DUSP6 upregulation obviated EGF and PKC-induced NKCC1 phosphorylation. NF-κB inhibition by PDTC prolonged ERK1/2 activation through GSK-3 inactivation leading to declines in DUSP1 expression levels. These results show that EGF receptor and PKC activation induce increases in HCEC proliferation through ERK1/2 interaction with NKCC1. This response is modulated by changes in DUSP1- and DUSP6-mediated negative feedback control of ERK1/2-induced NKCC1 phosphorylation.

Copyright © 2011 S. Karger AG, Basel

Introduction

Corneal epithelial cell renewal is essential for the maintenance of tissue transparency and visual acuity since tight junctional barrier function is preserved through this process. This function is required for suppressing pathogenic infiltration into the underlying stroma as well as maintaining the smooth corneal optical properties. This process is under autocrine and paracrine control by a host of cytokines. They interact with their cognate receptors in the basal proliferating layer to modulate and synchronize the events associated with epithelial turnover

Dr. Peter S. Reinach
Department of Biological Sciences, State University of New York
State College of Optometry, New York, NY 10036 (USA)
Tel. +1 212-938-5785, Fax +1 212-938-5794
E-Mail preinach@sunyopt.edu

[1, 2]. Receptor activation elicits through a myriad of interacting cell signaling pathways all of the responses that underlie epithelial renewal.

Epidermal growth factor (EGF) is a very efficacious promoter of cell proliferation and migration. Accordingly, much effort has been directed towards delineating the cell signaling pathways and transcription factors mediating EGF receptor (EGFR) control of these responses [3]. A number of studies indicate that EGFR activation elicits control of these responses through transient stimulation of a myriad of interacting cell signaling kinase pathways [4-6]. One aspect of this signaling process entails EGF stimulation of KCl cotransporters (KCC), K^+ channels and Na:K:2Cl cotransporter 1 (NKCC1) activity [7-9]. However, it is uncertain if ion transport stimulation leads to cell volume swelling and if NKCC1 phosphorylation is reflective of its activation by EGF. Furthermore, it is unclear how changes in the expression levels of dual specific protein phosphatases (DUSPs) that dephosphorylate ERK1/2 are modulated to control the mitogenic response to either EGFR or protein kinase C (PKC) stimulation.

EGF stimulates cell proliferation and migration through transient phosphorylation of the extracellular regulated kinase (ERK), p38 and JNK mitogen activated protein kinase (MAPK) pathways [6, 10]. In addition, the PI3-K/Akt/GSK pathway is activated, which has a negative feedback effect on the duration and magnitude of MAPK pathway activation. The extent of MAPK suppression is dependent on ERK, p38 MAPK and glycogen synthase kinase (GSK)-3α/β-mediated phosphorylation of different DUSPs that have variable MAPK substrate selectivity [11]. Gene microarray analysis of human corneal epithelial cells (HCEC) indicated that only DUSPs 1, 4, 5, and 6 are expressed at significant levels by these cells. DUSP6 is localized to the cytoplasm and is selective for ERK1/2 whereas DUSP5 is nuclear delimited and also selectively interacts with ERK1/2. On the other hand, DUSP1 and DUSP4 are more nonselective and modulate the patterns of activation of the terminal kinases in the ERK, p38 and JNK pathways. We validated DUSP5 and DUSP6 selectivity by showing in HCEC that DUSP5 knockdown with the appropriate short hairpin RNA (shRNA) augmented the mitogenic response to EGF as a consequence of sustained ERK1/2 phosphorylation. On the other hand, in a subline overexpressing DUSP6, this response was suppressed through inhibition of ERK1/2 phosphorylation status [4]. Subsequent to ERK1/2 activation by phosphorylation, NF-κB undergoes activation and nuclear translocation. In addition to ERK1/2 and p38 mediating in HCEC control of DUSP phosphorylation status, in enterocytes MKP-1 (i.e., DUSP1) expression is elicited by NF-κB [12]. However, such a feedback role for NF-κB has not been described in HCEC. Clarification of this question will provide additional insight into how to control the increases in cell proliferation and migration induced by EGFR or PKC stimulation.

Cell cycle progression and proliferation are dependent on specific changes in cell volume during different phases of the cell cycle [13, 14]. Swelling is needed to accommodate the increases in chromatin content for preserving its equivalence between the parental and daughter cells. In the corneal epithelium, the aforementioned increases in K^+ channel, KCC and NKCC1 activity occurring during cell cycle progression can also be induced during exposure to an anisoosmotic challenge resulting in activation of regulatory volume behavior by HCEC and rabbit corneal epithelial cells [7, 15-19]. Exposure to a hypertonic challenge initially induces shrinkage followed by restoration of isotonic volume due to stimulation of NKCC1 activity. Alternatively, swelling induced by exposure to a hypotonic challenge elicits shrinkage through increases in KCl efflux. Even though EGF stimulates NKCC1 activity in HCEC, it is unclear if its activation is sufficient to induce swelling subsequent to a regulatory volume decrease resulting from K^+ channel and KCC cotransporter activation.

The dependence of a mitogenic response on NKCC1 activation has been established in a number of tissues based on kinase-mediated increases in its phosphorylation status. Some of the kinases directly activating NKCC1 in dorsal root ganglion neurons are the sterile-20-like kinases (SPAK) and oxidative stress response-1 (OSR1) kinase. Upon their activation through phosphorylation by upstream kinases, SPAK and OSR1 bind and phosphorylate specific peptides on NKCC1 and stimulate its activity. Upstream from these kinases is the with-no-lysine (WNK1) kinase osmosensor. Independent of these kinases, there may be others that also activate the NKCC1. Some indication that other kinases may be involved is that the residues on the NKCC1 following protein kinase A (PKA) activation by forskolin are different than the targets of SPAK phosphorylation. Similarly, some of the WNK kinases may not be participants in mediating NKCC1 phosphorylation since expression of a WNK isoform mutant did not block hypertonic-induced PKCα-mediated NKCC1 phosphorylation (i.e., activation) [20]. More recently, it was shown in human airway epithelial

cells that PKCδ acted upstream of SPAK in the phosphorylation of the NKCC1 by hyperosmotic stress [21]. However, growth factors do not activate the endogenous WNK1 osmosensor. Therefore, the identity of the kinase mediating NKCC1 activation by growth factors remains elusive [22].

ERK pathway-dependent phosphorylation of this cotransporter has also been identified in rat heart and cardiomyocytes [23]. In HCEC, neither the extent of ERK1/2 interaction with NKCC1 induced by PKC or EGFR activation nor their cause and effect relationship has been described. Another question is whether or not EGF-induced intracellular calcium ($[Ca^{2+}]_i$) signaling is requisite for ERK pathway activation. Such a possibility exists since in HCEC EGF-induced increases in $[Ca^{2+}]_i$ influx through transient receptor potential canonical 4 (TRPC4) channels are required for the mitogenic response [24].

We show here in HCEC that both EGF and PKC-induced increases in cell proliferation are dependent on NKCC1-induced cell swelling that occur as result of ERK pathway-mediated phosphorylation of this cotransporter. This effect occurs through protein-protein interaction between ERK1/2 and NKCC1. As shown previously for EGF, the mitogenic response to PKC is also negatively regulated by cytoplasmic localized DUSP6 with high specificity for phospho-ERK1/2 (i.e., activated). These results show that control of DUSP6 stabilization through phosphorylation permits regulation of the magnitude of a cytokine-induced increase in cell proliferation. Another negative feedback mediator is NF-κB whose activation by EGF also modulates ERK1/2 activation through control of DUSP1 expression levels.

Materials and Methods

Materials

The R5 antibody to detect NKCC1 phosphorylation is a generous gift from B. Forbush (Yale University). The following antibodies were purchased from Cell Signaling Technology, Inc. (Beverly, MA): phospho-p38, phospho-SAPK/JNK, phospho-Ser 21/9 GSK-3α/β and rabbit polyclonal IgG. Anti-ERK1, phospho-ERK1/2, goat anti-mouse IgG-HRP, goat anti-rabbit IgG-HRP antibody, and anti-(H196) actin, anti-ERK1/2, anti-p38, and β-actin antibodies were purchased from Santa Cruz Biotechnology (Santa Cruz, CA). Calcein-AM was obtained from Invitrogen (Carlsbad, CA). Bumetanide, AG178, phorbol dibutyrate (PDBu), (1,2-Bis(2-aminophenoxy)ethane-N,N,N',N'-tetraacetic acid acetoxymethyl ester) (BAPTA/AM), PDTC (pyrroline dithiocarbamate), U0126, EGF, bovine insulin, gentamicin, and 0.05% trypsin-EDTA solution were purchased

from Sigma RBI (St. Louis, MO). Dulbecco's modified Eagle's medium (DMEM)/F12 medium and fetal bovine serum (FBS) were purchased from Gibco-Invitrogen (Carlsbad, CA).

Relative Cell Volume

Fluorescence was measured in HCEC after loading with 1 µM calcein-AM for 15 min at 23°C. Calcein-AM is a cell-permeable calcein derivative that is cleaved and trapped in the cytoplasm. Fluorescence was continuously measured with a 40x objective lens [oil immersion, numerical aperture (NA) 1.3] using a Nikon Diaphot inverted epifluorescence microscope equipped with halogen light source, calcein filter set (480-nm excitation, 490-nm dichroic mirror, 535-nm emission), photomultiplier detector, and 14-bit analog-to-digital converter. HCEC cultured on glass coverslips were secured in a perfusion chamber configured for rapid superfusion of a NaCl Ringers (306 mOsm) solution. It contained (mM): NaCl 147.8, KCl 4.7, $MgCl_2$ 0.4, glucose 5.5, $CaCl_2$ 1.8, and HEPES 5.3; pH adjusted to 7.4. Increases in fluorescence intensity were proportional to decline in osmolarity up to a 50% dilution with distilled water.

Western Blot analysis

Western blot experiments were performed as described [5]. In brief, the HCEC were gently washed twice in cold phosphate-buffered saline (PBS) and harvested in 0.5 ml cell lysis buffer. Cell lysates were centrifuged at 13,000 rpm for 15 min and supernates were collected. Protein content was measured with a bicinchoninic acid assay (BCA) protein assay kit (Pierce Biotechnology, Chicago, IL), and 200 µg protein was diluted with an equal volume of 2X Laemmli buffer. From 20 to 50 µg of denatured protein was electrophoresed on 10% polyacrylamide sodium dodecylsulfate (SDS) minigels and blocking polyvinylidene difluoride (PVDF) membranes with nonfat dry milk. The blots were exposed to the appropriate primary antibody overnight at 4°C. Then they were exposed to a 1:2000 dilution of a secondary antibody with anti-rabbit, anti-goat, or anti-mouse HRP labeled IgG for 1 h at room temperature. The immunoreactive bands were detected with a Western blot analysis kit (Amersham ECL Plus; GE Healthcare Lifesciences, Piscataway, NJ). Films were scanned and band density was quantified using image-conversion software (SigmaScan Pro 5.0; Systat Software, Inc., Mountain View, CA). The monoclonal anti-ERK1/2 and β-actin antibodies were used to test for protein loading equivalence.

Coimmunoprecipitation

Cells were lysed with lysis buffer and spun at 13,000 rpm for 10 min. An aliquot of supernatant containing 500 µg protein was exposed to either an antibody to detect total NKCC1 (i.e., T4), phosphorylated NKCC1 (i.e., R5) or total ERK1/2 antibody and gently agitated overnight at 4°C. The mouse monoclonal anti-NKCC ~T4 was purchased from DSHB (Developmental Studies Hybridoma Bank at the University of Iowa, Iowa City, IA). The T4 antibody binds the carboxy-110 terminus portion ~MET-902 to SER-1212 of human NKCC1 protein. Subsequently, protein A beads were added and cell lysates were exposed for another 2 h at 4°C with gentle agitation. Beads were washed a few times with PBS and cell lysis buffer. The

pellets obtained were resuspended in 50 µl cell lysis buffer, to which was added the same volume of 2X Laemmli buffer. The mixture was boiled for 5 min and then subjected to Western blot analysis with the appropriate antibody.

DUSP6 overexpression subline

This subline was previously established to determine the negative feedback effect of DUSP6 on EGF-induced increases in cytosolic ERK1/2 phosphorylation expression [4]. Stable overexpression of DUSP6 open reading frames (ORF) was accomplished using lentivectors based on the pLEX plasmid (Open Biosystems). The pLEX cassette drives expression of a MYC tagged ORF and the puror gene.

Cell Proliferation

[³H]-thymidine incorporation was performed as described [25]. After 24 h of serum starvation in medium supplemented with 0.5% bovine serum albumin, cells were incubated at 37°C for 1 h with 1 µCi/mL [³H]-thymidine (3.3-4.8 TBq/mmol) and then washed three times with ice-cold 5% trichloroacetic acid and twice with cold 90% ethanol. Cell lysates were solubilized with 0.2 N NaOH and 2% SDS. Radioactivity was monitored using a liquid scintillation counter and the data were normalized to cellular protein content using a modified Lowry assay.

Data Analysis

Data were analyzed using independent Student's two-tailed t-test. The data was considered significant if $p<0.05$. Results are reported as mean ± SEM for at least three independent experiments unless otherwise indicated.

Results

Dependence of proliferation on NKCC1 activation

In corneal epithelial cells, the mitogenic response to EGF occurs through stimulation of ion transporters and channel activity [8, 9]. To delineate if stimulation of NKCC1 by either EGF or a PKC activator, PDBu, is sufficient to induce this response, we determined their individual effects on cell proliferation. Figure 1 shows that during exposure to either 10 ng/ml EGF or 1 µM PDBu, proliferation increased about 1.6 or 1.72-fold, respectively whereas 30 min preincubation with 50 µM bumetanide fully inhibited each of these responses indicating that the mitogenic response to EGF is dependent on NKCC1 activation.

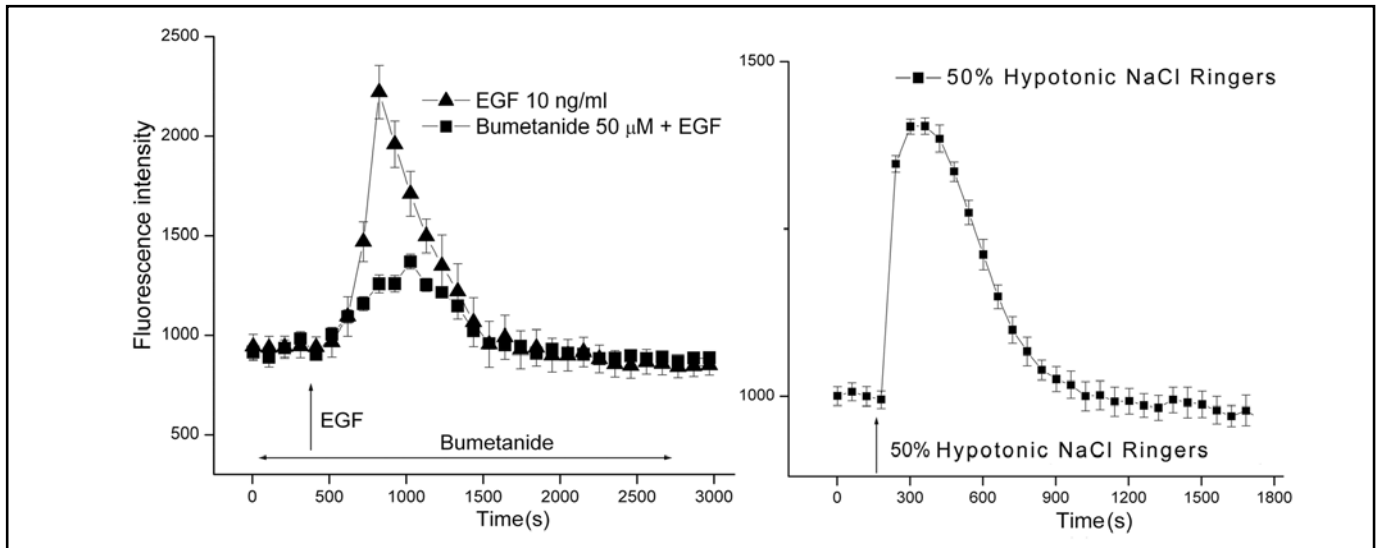### NKCC1 activation induces transient swelling

Even though it is apparent that NKCC1 activation is requisite for EGF and PKC-induced mitogenesis, it was unclear if its increase in activity is associated with cell swelling. To make this assessment, we determined if
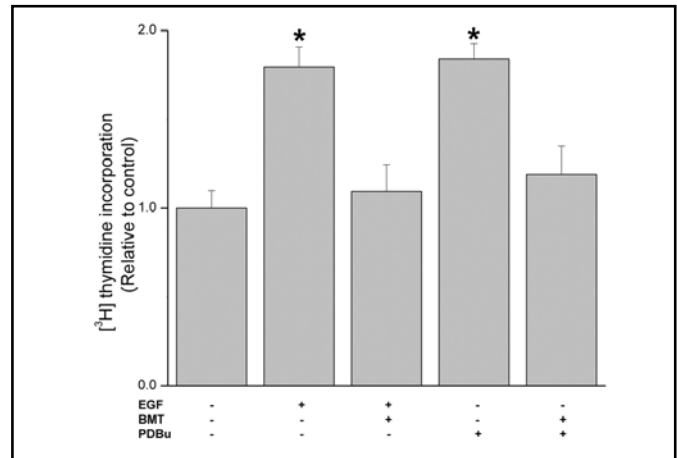
Fig. 1. NKCC1 inhibition suppresses EGF and PDBu-induced increases in cell proliferation. HCEC were pretreated for 30 min with bumetanide (BMT; 50 µM) and in some conditions were then exposed for an additional 20 h to either PDBu (1 µM) or EGF (10 ng/ml). Cells were incubated for 1 h with 1 µCi/mL [³H]-thymidine. Protein content was determined with a BCA protein assay kit. Data are presented as mean ± SEM (n=3). * p < 0.05 versus untreated control.

relative cell volume increased during exposure to 10 ng/ml EGF. Figure 2 (left panel) shows that after about 7 min calcein emitted fluorescence increased more than 2-fold (Mean ± SEM: n=5; p<0.001 versus untreated control) followed by a return to a baseline value after about 12 min. On the other hand, 30 min preexposure to 50 µM bumetanide suppressed this rise by 68% showing that NKCC1 activation contributes to this response. The inability of bumetanide to fully suppress EGF-induced swelling may be indicative of a contribution by an increase in Na:H exchanger activity to this response since EGF-induces swelling in some other epithelia by stimulating Na⁺ influx via this pathway.

We validated that the EGF-induced rise in fluorescence is reflective of swelling by exposing the cells to a 50% hypotonic challenge. Such a stress induces a regulatory volume decrease response leading initially to a decrease in cell volume below the isotonic volume. This decline occurs in HCEC as a consequence of a net loss of KCl mediated by stimulation of K⁺ channel activity and KCC activity [7, 8, 19]. Isotonic volume is eventually restored subsequent to a volume overshoot below the isotonic volume. This occurs through NKCC1 activation [16]. Figure 2 (right panel) shows that the transient increase in fluorescence intensity induced by EGF was mimicked by exposure to a 50% hypotonic challenge. Therefore, this response induced by EGF is reflective of transient cell swelling.

Fig. 2. EGF induces transient HCEC swelling through NKCC1 activation. Calcein loaded HCEC attached to coverslips were placed in a chamber for superfusion of room temperature NaCl Ringers from syringes onto the stage of an epifluorescent microscope. The epifluorescent emission was measured between 503 and 530 nm. Panel A shows that following signal stabilization of about 3 min during control superfusion, the solution was substituted for another containing 10 ng/ml EGF (↑) (Mean ± SEM: n=5 coverslips; p<0.001 versus untreated control). After about 3 min, the corrected signal nearly rapidly doubled followed by gradual decline to reach a baseline level after about 15 more min. Pre-exposure for 30 min to 50 µM bumetanide suppressed the subsequent EGF-induced transient by about 70% (n=5; p<0.001). Panel B shows that substitution of the control 306 mOsm NaCl Ringers with one diluted by 50% induced after about 1 min a transient increase in fluorescence reflective of swelling since calcein is a self-quenching dye (n=4 coverslips; p<0.005 versus isotonic control). The pattern of this transient was very similar to that induced by EGF, but instead is reflective of hypotonic-induced stimulation of KCC and K$^+$ channel activity rather than NKCC1 activation by EGF shown in panel A [7, 17].
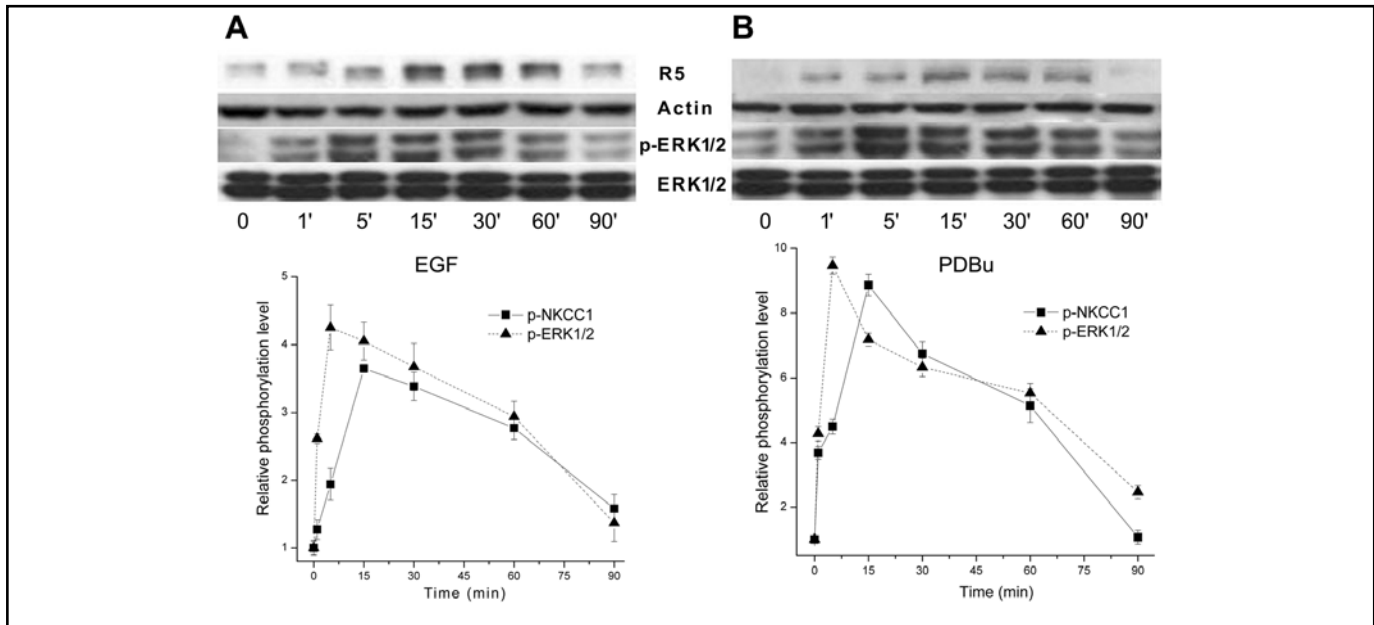
Time dependent increases in NKCC1 phosphorylation induced by EGF and PDBu

It is well established that NKCC1 phosphorylation by different kinases mediates activation of this cotransporter [21]. Nevertheless, in fibroblasts there is some uncertainty regarding the cause and effect relationship between ERK1/2 and NKCC1 activation since it was reported that growth factor-induced NKCC1 activation precedes ERK1/2 phosphorylation [26]. However, ERK1/2 and PKCδ activation induced NKCC1 phosphorylation in human tracheal epithelial cells [21]. We also used a R5 phospho-specific antibody to determine the time dependence for changes in NKCC1 phosphorylation. R5 was raised to detect phosphorylation of residues Thr212 and Thr217 in human NKCC1 [27]. As the pathways mediating ERK1/2 phosphorylation by EGF and phorbol esters are different from one another [28], the time patterns were also determined of changes in p-ERK1/2 and p-NKCC1 levels induced by 1 µM PDBu. Figure 3A shows that after 5 min exposure to EGF phosphorylation of ERK1/2 increased nearly 4.7-fold, remained essentially stable until 30 min and waned to reach at 90 min a level similar to the baseline value. After 15 min, NKCC1 phosphorylation increased to a level similar to that reached by ERK1/2 at 5 min. Subsequently, the NKCC1 level waned faster, but stabilized at a value at 90 min that was nearly 2-fold higher than that for ERK1/2. Figure 3B shows that PKC stimulation induced a similar pattern of increases in ERK1/2 and NKCC1 phosphorylation. The level of p-ERK1/2 increased rapidly to reach a maximum value after 5 min followed by declines reaching nearly the baseline level after 90 min. Changes in p-NKCC1 mirrored those for p-ERK1/2. However, the maximum p-NKCC1 level was observed 10 min later than those for ERK1/2. This close association between the time-dependent changes in p-ERK1/2 and p-NKCC1 induced by either EGF or PDBu appears to indicate that ERK1/2 mediates NKCC1 activation.

Dependence of NKCC1 phosphorylation on ERK1/2 activation

Figure 4A documents that the increases in ERK1/2 and NKCC1 phosphorylation were indeed dependent on EGF-induced EGFR and ERK1/2 activation since inhibition for 5 min of EGFR or Mek1/2 activation with either 5 µM AG1478 or 10 µM U0126, respectively blocked EGF-induced increases in both p-ERK1/2 and

Fig. 3. Time-dependent changes in ERK1/2 and NKCC1 phosphorylation status induced by EGF and PDBu. HCEC were serum starved for 24 h at 80% to 90% confluence. Panel A shows the effects of exposure to 10 ng/ml EGF for up to 90 min with a representative Western blot analysis of anti-phosphor p-NKCC1 (i.e., R5) and p-ERK1/2 antibody binding. Panel B shows cells exposed to 1 µM PDBu and Western blot analysis performed using the same antibodies as those shown in panel A. Equal loading of proteins was confirmed by reprobing the blots with β-actin.

p-NKCC1 formation. In addition, these results indicate that EGF-induced NKCC1activation is completely ERK pathway-dependent. To clarify whether or not ERK1/2 phosphorylation is a result or a cause of NKCC1 activation, we determined the cause and effect relationship between NKCC1 and ERK1/2 activation by comparing the effects of either 25 or 50 µM bumetanide on EGF-induced NKCC1 and ERK1/2 phosphorylation (Fig. 4B). Preinhibition for 30 min with either 25 or 50 µM bumetanide abolished the EGF-induced increases in NKCC1 phosphorylation status, but had no effect on ERK1/2 activation. Taken together, NKCC1 activation occurred as a consequence of ERK1/2 activation.

PKC mediates NKCC1 phosphorylation through ERK1/2 activation

We determined if the cause and effect relationship between ERK1/2 and NKCC1 activation by PKC is the same as that for EGF. Figure 5 compares the individual effects of 50 µM bumetanide or 10 µM U0126 on PDBu-induced ERK1/2 and NKCC1 phosphorylation. A 30 min preincubation with bumetanide completely blocked a near 6-fold increase in NKCC1 phosphorylation, but had only an insignificant effect on the 7.4-fold increase in ERK1/2 phosphorylation induced by PDBu. On the other hand, preincubation with U0126 completely abolished both PDBu-induced ERK1/2 and NKCC1 activation. This
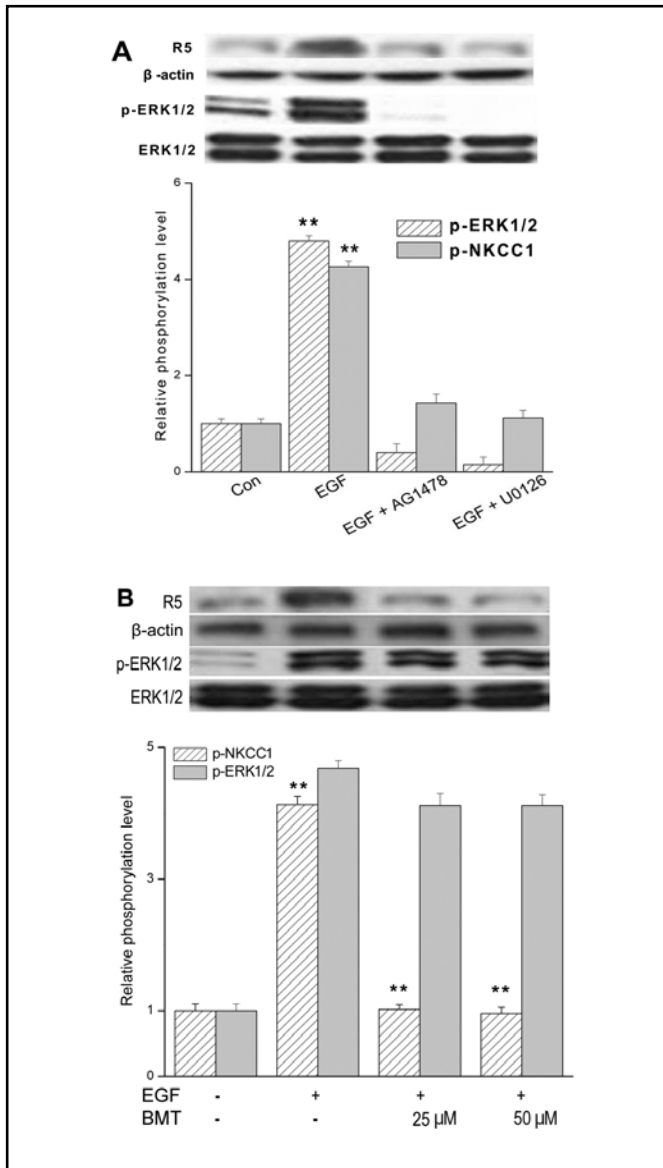
difference indicates that PKC-induced NKCC1 activation is completely dependent on Mek1/2-mediated ERK1/2 phosphorylation whereas bumetanide failed to block ERK1/2 activation by PKC.

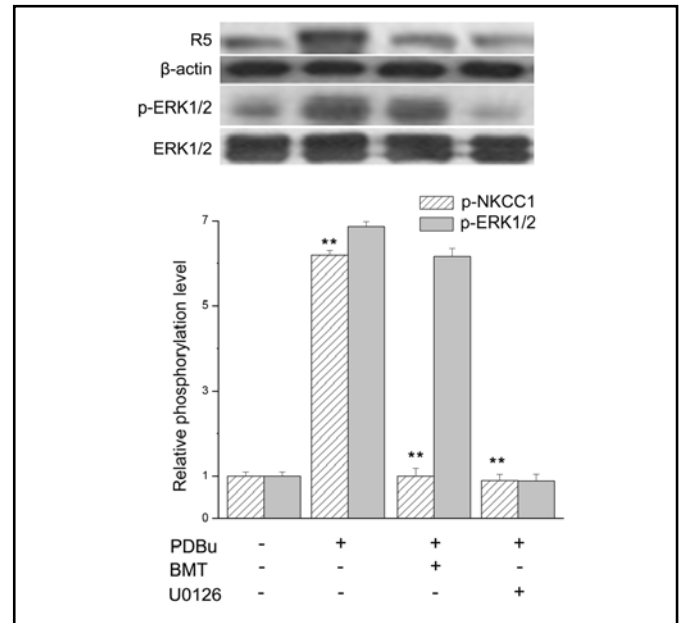*Dependence of ERK1/2 activation by EGF on Ca^{2+} influx*

EGF-induced increases in HCEC proliferation are dependent on its activation of plasma membrane Ca^{2+} influx through one isotype of the TRP canonical superfamily designated TRPC4 [24]. We determined if EGF-induced ERK1/2 and NKCC1 phosphorylation is dependent on cytosolic $[Ca^{2+}]_i$ content. Figure 6 shows that large increases in the phosphorylation level of both proteins caused by 10 ng/ml EGF at 5 min similarly waned as a function of increases in BAPTA-AM concentration (unstimulated control level not shown). With 120 µM BAPTA-AM, EGF-induced ERK1/2 and NKCC1 phosphorylation was fully attenuated. This result suggests that there is a direct dependence between ERK1/2 and NKCC1 activation on transient rises in $[Ca^{2+}]_i$ levels induced by EGF.

EGF-induces ERK1/2-NKCC1 interaction

To determine if ERK1/2 activation elicits a close association with NKCC1, we probed for time-dependent increases in protein-protein interaction between them.
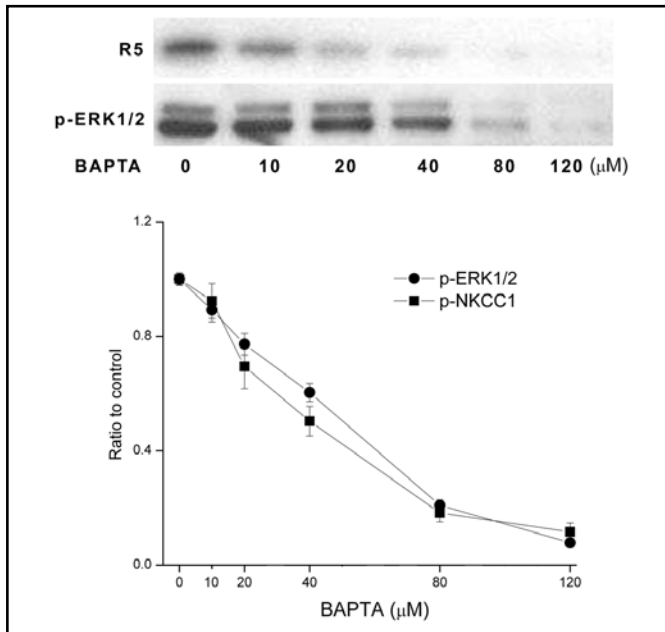
Fig. 5. Inhibition of PDBu-induced PKC activation of NKCC1 and ERK1/2 phosphorylation. HCEC were serum starved for 24 h at 80% to 90% confluence. Representative Western blot analysis comparing the effects of exposure to 1 μM PDBu in the presence and absence of either 50 μM bumetanide (BMT) (**$p<0.001$ PDBu versus treat with BMT). or 10 μM U0126 (**$p<0.001$ PDBu versus treat with U0126 on phosphorylation levels in both NKCC1 and ERK1/2). on p-NKCC1 and p-ERK1/2 detected with anti p-NKCC1 (i.e., R5) and p-ERK1/2 antibodies. Equivalent protein loading was confirmed by reprobing the same blot with anti actin and ERK1/2 antibody, respectively. Data represent the mean ± SEM of three independent experiments.

First, we assessed if there are any changes in the amounts of p-ERK1/2 associated with total NKCC1 during EGF exposure. Membrane enriched fractions of EGF stimulated cells were subjected to SDS polyacrylamide gel electrophoresis. A representative image shown in Figure 7 (insert) indicates that EGF caused a time-dependent increase in amounts of both NKCC1 (upper band) and phospho-ERK1/2 (lower band) in the same fraction. The summary plot shows that their content changed with a similar pattern and after 15 min rose about 2.3 or 5-fold for NKCC1 or p-ERK1/2, respectively. This parallelism suggests that during stimulation of the resting cells with EGF an interaction occurred between phosphorylated ERK1/2 and membrane associated NKCC1.
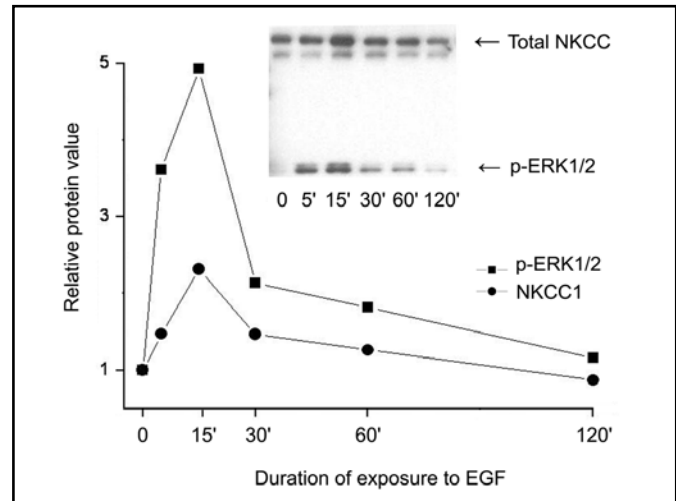
Dose dependent effects of EGF on ERK1/2-NKCC1 interaction

To validate protein-protein interaction between phosphorylated ERK1/2 and total NKCC1, pull down

Fig. 4. Dependence of NKCC1 activation on EGFR-linked signaling. HCEC were serum starved for 24 h at 80% to 90% confluence. (A) Representative Western blot analysis comparing the effects of exposure to 10 ng/ml EGF after a 5 min exposure in the presence and absence of either 5 μM AG1478 or 10 μM U0126 on ERK1/2 and NKCC1 phosphorylation (n=3; **$p<0.001$ versus untreated control). The blots were probed with anti p-NKCC1 (i.e., R5) and p-ERK1/2 antibodies. Equal loading of proteins was confirmed by reprobing the same blot with anti total ERK1/2 antibody. Summary of changes in ERK1/2 and NKCC1 phosphorylation status is shown below the aforementioned blots. (B) Representative experiments of the dose-dependent inhibitory effects of 25 to 50 μM bumetanide (BMT) with 10 ng/ml EGF-induced NKCC1 phosphorylation detected with the anti p-NKCC1 and p-ERK1/2 antibodies (n=3; **$p<0.001$ versus NKCC1 phosphorylation levels treated with BMT). Equivalent protein loading was confirmed by reprobing the same blot with actin and ERK1/2 antibody, respectively. Data represent the mean ± SEM of three independent experiments.

Fig. 6. Dependence of EGF-induced ERK1/2 and NKCC1 phosphorylation on $[Ca^{2+}]_i$. HCEC were serum starved for 24 h at 80% to 90% confluence. Representative Western blot analysis compares the dose dependent inhibitory effects of exposure to BAPTA on 10 ng/ml EGF-induced p-NKCC1 and p-ERK1/2 formation detected with the anti p-NKCC1 (i.e., R5) and p-ERK1/2 antibodies. HCEC were preincubated for 30 min with each of the indicated BAPTA concentrations prior to exposure to EGF for an additional 5 min. Results were normalized to the increase in p-ERK1/2 formation obtained after 5 min in the absence of BAPTA. Data represent the mean ± SEM of three independent experiments (at concentrations over 40 μM BAPTA, p<0.001 versus untreated control).
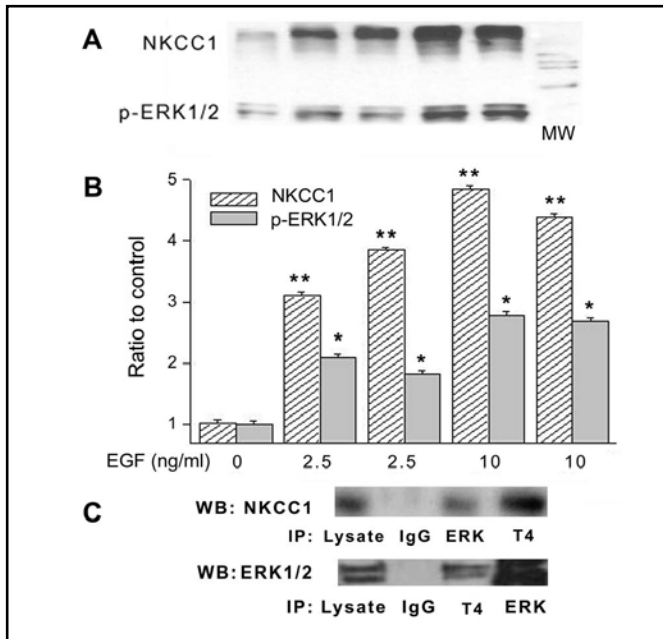

Fig. 7. Time-dependent changes in p-ERK1/2 association with NKCC. HCEC were serum starved for 24 h at 80% to 90% confluence. Cells were exposed to 10 ng/ml EGF for up to 120 min. Membrane-enriched fractions were obtained following centrifugation. Pellets were probed for relative amounts of total NKCC1 with the anti T4 antibody and p-ERK1/2 antibodies at the indicated times following exposure to EGF. Data represent the mean ± SEM of three independent experiments (after 15 min exposure to EGF, p<0.002 total NKCC versus untreated control; or p<0.001 p-ERK1/2 versus untreated control, respectively). The error bars fall within the range of the indicated symbols for p-ERK1/2 and NKCC1.

experiments with a specific p-ERK1/2 antibody were performed. Figure 8A demonstrates that EGF caused concentration-dependent increases in the amounts of association of NKCC1 with p-ERK1/2. Figure 8B provides a summary of the results obtained with duplicate samples each performed in triplicate that were exposed to 2.5 or 10 ng/ml EGF. There is a clear correspondence between increases in p-ERK1/2 and total NKCC1 in cell extracts, which rose with 10 ng/ml EGF up to 4 and 8-fold, respectively. This association between p-ERK1/2 and NKCC1 levels suggests that p-ERK1/2 co-localized with NKCC1 and could be one of the kinases directly involved in EGF-induced NKCC1 activation. To further validate their colocalization, we immunoprecipitated NKCC1 and probed the immune complexes for p-ERK1/2 and vice versa. The results shown in Fig. 8C demonstrate that there was a significant amount of NKCC1 in the immune complexes of ERK1/2 (top panel) and similarly ERK1/2 was found in the NKCC1 complexes (bottom panel). These results also strongly support that protein-

protein interaction occurred between p-ERK1/2 and NKCC1.

Negative feedback control by DUSP6 of ERK1/2 activation

The mitogenic responses in HCEC to EGFR and PKC stimulation are dependent on the duration and magnitude of ERK1/2 activation [6]. DUSP6 inactivates p-ERK1/2 through dephosphorylating serine and threonine residues on this terminal kinase. We determined if DUSP6 overexpression in a subline altered the effects of EGFR or PKC activation on NKCC1, p38, JNK1/2 and ERK1/2 phosphorylation status. Figure 9 contrasts in each case the difference between the individual effects of 15 min exposure to either EGF or PDBu on each of the aforementioned entities. In control cells, 15 min exposure to either EGF or PDBu led to increases in phosphorylation status of all kinases whereas in the DUSP6 overexpressing cell line only increases in ERK1/2 and NKCC1 phosphorylation were completely suppressed. Such suppression fully obviated increases in cell proliferation induced by PKC stimulation with 1 μM PDBu (data not shown). These effects indicate that ERK1/2 inactivation blocks NKCC1 phosphorylation.
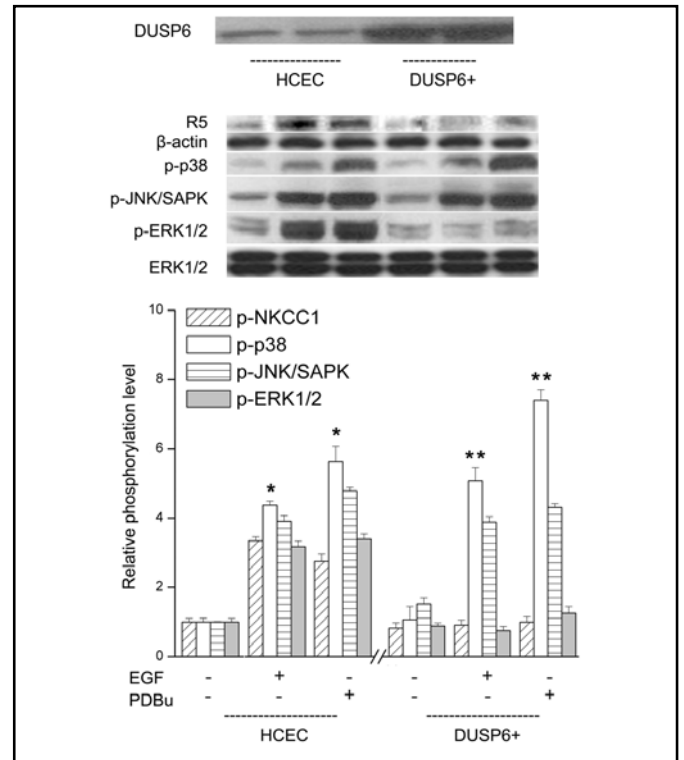
Fig. 8. Pull-down experiments validate NKCC1-p-ERK1/2 interaction induced by EGF. HCEC were serum starved for 24 h at 80% to 90% confluence. (A) Cells were exposed to either 2.5 or 10 ng/ml EGF for 10 min. Membrane enriched pellets were obtained from different cell lysates and Western blot (WB) probing for either p-ERK1/2 or total NKCC1 association with p-ERK1/2 and T4 antibodies, respectively. (B) Results of experiments performed in duplicate at each concentration normalized to the amounts detected prior to exposure to EGF (Exposure to 2.5 or 10 ng/ml EGF, *$p<0.05$ p-ERK1/2 versus untreated control; **$p<0.001$ NKCC1 versus untreated control). (C) Co-localization validation entailed immunoprecipitation (IP) with beads bound to ERK1/2 or NKCC1 followed by probing the precipitate with either anti T4 or ERK1/2 antibodies using Western blot analysis. In the IPs obtained with either the anti T4 antibody or ERK1/2 antibody, there are increases in the amounts of ERK1/2 and NKCC1, respectively. These results validate that exposure to EGF-induces increases in the amounts of p-ERK1/2 associating with NKCC1. Cells were exposed to 10 ng/ml EGF for 10 min. The results shown were obtained from two different experiments each performed in triplicate.

Fig. 9. Selective inhibition in DUSP6 overexpression HCEC subline (DUSP6+) of EGF and PDBu -induced ERK1/2 and p-NKCC1 phosphorylation. HCEC were serum starved for 24 h at 80% to 90% confluence. Representative Western blot analysis compares p-NKCC1, p-p38, p-JNK1/2/SAPK and p-ERK1/2 formation with the appropriate antibody in cell lysates obtained from wildtype and the DUSP6 overexpressing HCEC subline. Summaries of the individual effects of DUSP6 overexpression are shown below of data (mean ± SEM: n=3; *$p<0.05$ versus untreated control) obtained from three individual experiments. DUSP6 overexpression selectively blocked EGF and PDBu-induced p-NKCC1 and p-ERK1/2 (n=3; **$p<0.001$ versus EGF and PDBu-induced p-p38 and p-JNK1/2/SAPK), which is consistent with the notion that NKCC1 phosphorylation is dependent on ERK1/2 activation by either EGF or PDBu.

NF-κB inactivation by PDTC destabilizes DUSP1 expression

The phosphorylation status of DUSPs affects their stability, which in turn modulates through negative feedback the duration and magnitude of ERK1/2 activation and the resulting mitogenic response to a growth factor [29]. As ERK1/2 and GSK-3α/β mediate DUSP1 phosphorylation, changes in DUSP1 expression levels shape the duration and magnitude of both ERK1/2 and p38 phosphorylation [5, 6]. Such shaping has not been shown to be related to changes in DUSP activity, but rather DUSPs stabilization is modulated through changes in their phosphorylation status [30]. It was recently shown in enterocytes that DUSP1 stabilization is also affected by NF-κB activation, which in turn has a negative feedback effect on p38-induced phosphorylation [12].

We determined if NF-κB inhibition by 50 μM PDTC affects EGF-induced changes in NKCC1, ERK1/2 and GSK-3α/β phosphorylation as well as total DUSP1 expression. To make such an assessment, HCEC were preincubated with PDTC followed by 15 min exposure to 10 ng/ml EGF. Figure 10 compares the effects of EGF alone at 15 min with those of exposure to EGF for up to 90 min in the presence of PDTC. With EGF alone, the DUSP1 level was much higher than that in the presence of both EGF and PDTC. Such a difference was associated

with higher levels of phosphorylated NKCC1, ERK1/2 and GSK-3α/β than those obtained in the absence of PDTC. It should be recalled that an increase in GSK-3α/β phosphorylation is reflective of inhibition of this kinase. Interestingly, the elevated levels of p-GSK-3α/β were accompanied by a marked decline in DUSP1 expression levels over a 90 min period. This decline in DUSP1 expression is attributable to EGF-induced inactivation of GSK-3α/β through its activation of the PI3-K/Akt/GSK-3 pathway in HCEC [6]. The accompanying stabilization of the increase in EGF-induced ERK1/2 phosphorylation is therefore accountable for by loss of DUSP1 stabilization resulting from PDTC promotion of GSK-3α/β inactivation (i.e., sustained phosphorylation).

Discussion

In HCEC, some of the downstream signaling events induced by EGFR stimulation include transient activation of the MAPK superfamily as well as the PI3-K/Akt signaling cascade, PKC and time-dependent stimulation of K^+ channel, KCC along with increases in NKCC1 activity [7-9, 31-33]. All of these changes are linked to NF-κB activation whose p50/p65 subunits induce promoter activation leading to the expression of genes underlying proliferation [3]. MAPK activation is under the negative feedback control elicited by DUSPs 1, 4, 5 and 6 whose stabilization by kinases is phosphorylation-dependent [4, 30]. The goal of the current study was to: 1) better delineate the interdependence between the aforementioned signaling events in modulation of EGF and PKC-induced mitogenesis; 2) clarify how changes in DUSPs 1 and 6 expression levels elicit negative feedback control of ERK1/2-induced NKCC1 activation.

Even though earlier studies showed that modulation of NKCC1 activity affects mitogen-induced increases in cell proliferation, there was no evidence indicating that swelling is attributable to its stimulation [9, 16]. Here we show (Fig. 2: left panel) that EGF induced transient increases in apparent cell volume, which were associated with ERK1/2-induced NKCC1 phosphorylation. This cause and effect relationship is in agreement with a study using mice astrocytes in which exposure to a high K^+ containing medium induced swelling that is dependent on ERK1/2 activation of NKCC1[34]. The changes induced by PKC activation are also supportive of this cause and effect relationship. This is evident since PDBu, whose effects may not be limited to PKC activation, induced a
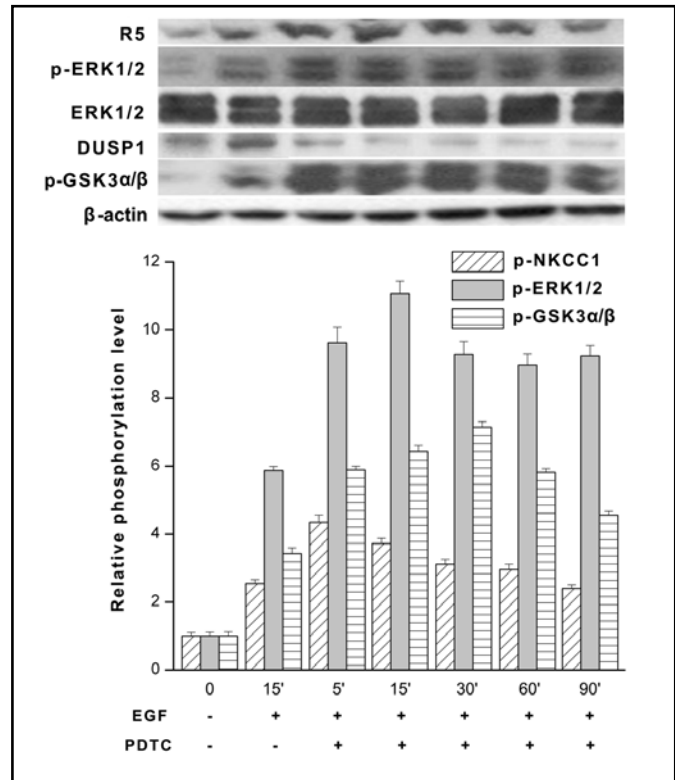
Fig. 10. NF-κB inhibition prolongs EGF-induced ERK1/2 activation through downregulation of DUSP1 expression. HCEC were serum starved for 24 h at 80% to 90% confluence. Cells were exposed to 10 ng/ml EGF either in the presence or absence of 50 μM PDTC and cell lysates were obtained at each of the indicated times up to 90 min. The results obtained with PDTC following 15 min incubation and exposure to EGF for another 15 min are compared to those with EGF for up to 90 min without PDTC. Western blot analysis was performed with p-NKCC1, p-ERK1/2 and equivalent protein loading was confirmed with the anti ERK1/2 antibody. Under the same conditions individual changes in DUSP1 and p-GSK-3α/β expression detected with the appropriate antibody. Data represent the mean ± SEM of three independent experiments. It is notable that PDTC exposure resulted in sustained p-ERK1/2 and p-NKCC1 formation over the 90 min ($p<0.001$ versus untreated control) period whereas declines in total DUSP1 exposure were accompanied by pronounced and continuous p-GSK3-α/β expression ($p<0.05$ versus untreated control). PDTC appears to inhibit GSK-3α/β through phosphorylation leading to declines in DUSP1 expression. Such declines account for sustained ERK1/2 phosphorylation due to loss of negative feedback control by DUSP1 of ERK1/2 activation.

maximal increase in ERK1/2 phosphorylation after the first 5 min whereas an increase in NKCC1 phosphorylation status reached its peak only after 15 min (Fig. 3). Furthermore, the subsequent decreases in the phospho-NKCC1 levels mirrored those of phospho-ERK1/2.

It should be mentioned that an increase in NKCC1 phosphorylation status detected with the R5 antibody might not necessarily be reflective of a corresponding change in its ion transport activity. Recently, it was shown in HEK-293 cells expressing NKCC1 that increases in its phosphorylation status detected with this antibody were not in all cases accompanied by ion transport activity stimulation. This disconnect led to the conclusion that NKCC1 phosphorylation is necessary, but not sufficient for inducing ion transport stimulation. Nevertheless, the R5 antibody provided meaningful results showing that declines in NKCC1 phosphorylation status were associated with proportional decreases in ion transport activity [35].

In some other tissues, growth factors and hypertonic stress initially induce NKCC1 activation through either PKC phosphorylation or ERK1/2 phosphorylation [20, 21, 23]. In HCEC, ERK pathway inhibition also eliminated increases in ERK1/2 and NKCC1 phosphorylation status induced by PDBu. Both of these events appear to be dependent on EGF-induced rises in $[Ca^{2+}]_i$ since the declines in their activation mirrored one another as a function of increases in BAPTA-AM concentration (Fig. 6). This dependence of MAPK activation on Ca^{2+} influx induced by EGF was described in conjunctival goblet cells and mice astrocytes [36, 34].

Even though we found that EGF induced time- and concentration-dependent increases in the interaction between phospho-ERK1/2 and total NKCC1 in membrane enriched fractions (Figs. 7 and 8), these results do not indicate whether phospho-ERK1/2 directly activates NKCC1. Nevertheless, NKCC1 phosphorylation is dependent on ERK1/2 activation by either EGF or PDBu since DUSP6 overexpression (Fig. 9) only blocked NKCC1 and ERK1/2 phosphorylation. Phosphorylation of NKCC1 by SPAK and OSR1 kinases is downstream from ERK1/2 in other tissues and is critical in NKCC1 activation. These kinases induce NKCC1 activation in response to cell shrinkage, injury and other effectors, but not growth factors [22]. They may not have redundant function, but are individually activated by different upstream signaling pathways. For example, in dorsal root ganglion neurons SPAK and OSR1 both mediate NKCC1 phosphorylation whereas in different tissues their direct involvement in this process is variable [20]. In any case, the identity remains elusive of the kinases directly mediating ERK1/2-induced NKCC1 phosphorylation.

The results shown in Fig. 10 indicate that DUSP1 expression is also modulated by changes in NF-κB activity as well as the ERK1/2 and PI3-K/Akt/GSK-3 pathway. This is evident since PDTC caused DUSP1 expression to decline resulting in sustained and prolonged phosphorylation of ERK1/2 and GSK-3α/β as well as larger increases in p-NKCC1 formation. This change in the ERK1/2 phosphorylation pattern suggests that PDTC also inhibits GSK-3α/β since its inhibition by a GSK-3α/β inhibitor, SB415286, caused DUSP1 expression to wane with the same time course as that shown here [6]. This waning effect following GSK-3α/β inhibition by phosphorylation occurred because active nonphosphorylated GSK-3α/β mediates DUSP1 phosphorylation, which protects DUSP1 from being degraded by endosomal activity. Our finding that PDTC inhibited GSK-3α/β dephosphorylation is consistent with two different reports in which: 1) this antioxidant reduced hypoxia-induced Akt and GSK-3α/β dephosphorylation in the brain [37]; 2) PDTC-induced GSK-3α/β inactivation in enterocytes resulting in prolonged MAPK activation [12].

Taken together, this study suggests that EGF and PKC-induced increases in proliferation are essentially dependent on increases in $[Ca^{2+}]_i$ levels mediating p-ERK1/2-induced NKCC1 phosphorylation through protein-protein interaction between ERK1/2 and NKCC1. The mitogenic responses induced by such interaction are modulated through negative feedback control by changes in the expression levels of DUSP1 and DUSP6. DUSP1 expression levels are determined by changes in NF-κB activity as well as previously described modulation of ERK1/2 and p38 MAPK phosphorylation [6].

Acknowledgements

References

1   Yu FS, Yin J, Xu K, Huang J: Growth factors and corneal epithelial wound healing. Brain Res Bull 2010;81:229-235.

2   Reinach PS, Pokorny KS: The corneal epithelium: Clinical relevance of cytokine-mediated responses to maintenance of corneal health. Arq Bras Oftalmol 2008;71:80-86.

3   Lu L, Wang L, Li T, Wang J: Nf-kappab subtypes regulate ccctc binding factor affecting corneal epithelial cell fate. J Biol Chem 2010;285:9373-9382.

4 Wang Z, Reinach PS, Zhang F, Vellonen KS, Urtti A, Turner H, Wolosin JM: Dusp5 and dusp6 modulate corneal epithelial cell proliferation. Mol Vis 2010;16:1696-1704.

5 Wang Z, Yang H, Tachado SD, Capo-Aponte JE, Bildin VN, Koziel H, Reinach PS: Phosphatase-mediated crosstalk control of Erk and p38 mapk signaling in corneal epithelial cells. Invest Ophthalmol Vis Sci 2006;47:5267-5275.

6 Wang Z, Yang H, Zhang F, Pan Z, Capo-Aponte J, Reinach PS: Dependence of EGF-induced increases in corneal epithelial proliferation and migration on GSK-3 inactivation. Invest Ophthalmol Vis Sci 2009;50:4828-4835.

7 Capo-Aponte JE, Wang Z, Akinci MA, Wolosin JM, Pokorny KS, Iserovish P, Reinach PS: Potassium-chloride cotransporter mediates cell cycle progression and proliferation of human corneal epithelial cells. Cell Cycle 2007;6:2709-2718.

8 Roderick C, Reinach PS, Wang L, Lu L: Modulation of rabbit corneal epithelial cell proliferation by growth factor-regulated K$^+$ channel activity. J Membr Biol 2003;196:41-50.

9 Yang H, Wang Z, Miyamoto Y, Reinach PS: Cell signaling pathways mediating epidermal growth factor stimulation of Na:K:Cl cotransport activity in rabbit corneal epithelial cells. J Membr Biol 2001;183:93-101.

10 Okada Y, Saika S, Shirai K, Yamanaka O, Kitano A, Wang Z, Yang H, Reinach P: JNK MAPK signaling contributes in vivo to injury-induced corneal epithelial migration. Ophthalmic Res 2009;42:185-192.

11 Owens DM, Keyse SM: Differential regulation of map kinase signalling by dual-specificity protein phosphatases. Oncogene 2007;26:3203-3213.

12 Wang J, Ford HR, Grishin AV: NF-kappab-mediated expression of MAPK phosphatase-1 is an early step in desensitization to tlr ligands in enterocytes. Mucosal Immunol 2010;3:523-534.

13 Hoffmann EK, Lambert IH, Pedersen SF: Physiology of cell volume regulation in vertebrates. Physiol Rev 2009;89:193-277.

14 Lang F, Foller M, Lang K, Lang P, Ritter M, Vereninov A, Szabo I, Huber SM, Gulbins E: Cell volume regulatory ion channels in cell proliferation and cell death. Methods Enzymol 2007;428:209-225.

15 Bildin VN, Wang Z, Iserovich P, Reinach PS: Hypertonicity-induced p38MAPK activation elicits recovery of corneal epithelial cell volume and layer integrity. J Membr Biol 2003;193:1-13.

16 Bildin VN, Yang H, Crook RB, Fischbarg J, Reinach PS: Adaptation by corneal epithelial cells to chronic hypertonic stress depends on upregulation of Na:K:Cl cotransporter gene and protein expression and ion transport activity. J Membr Biol 2000;177:41-50.

17 Capo-Aponte JE, Iserovich P, Reinach PS: Characterization of regulatory volume behavior by fluorescence quenching in human corneal epithelial cells. J Membr Biol 2005;207:11-22.

18 Capo-Aponte JE, Wang Z, Bildin VN, Pokorny KS, Reinach PS: Fate of hypertonicity-stressed corneal epithelial cells depends on differential MAPK activation and p38 MAPK/Na-K-2Cl cotransporter1 interaction. Exp Eye Res 2007;84:361-372.

19 Wu X, Yang H, Iserovich P, Fischbarg J, Reinach PS: Regulatory volume decrease by sv40-transformed rabbit corneal epithelial cells requires ryanodine-sensitive Ca^{2+}-induced Ca^{2+} release. J Membr Biol 1997;158:127-136.

20 Delpire E, Gagnon KB: Spak and osr1, key kinases involved in the regulation of chloride transport. Acta Physiol (Oxf) 2006;187:103-113.

21 Smith L, Smallwood N, Altman A, Liedtke CM: Pkcdelta acts upstream of SPAK in the activation of NKCC1 by hyperosmotic stress in human airway epithelial cells. J Biol Chem 2008;283:22147-22156.

22 Kahle KT, Rinehart J, Lifton RP: Phosphoregulation of the Na-K-2Cl and K-Cl cotransporters by the wnk kinases. Biochim Biophys Acta 2010;1802:1150-1158.

23 Andersen GO, Skomedal T, Enger M, Fidjeland A, Brattelid T, Levy FO, Osnes JB: Alpha1-ar-mediated activation of nkcc in rat cardiomyocytes involves Erk-dependent phosphorylation of the cotransporter. Am J Physiol Heart Circ Physiol 2004;286:H1354-1360.

24 Yang H, Mergler S, Sun X, Wang Z, Lu L, Bonanno JA, Pleyer U, Reinach PS: TRPC4 knockdown suppresses epidermal growth factor-induced store-operated channel activation and growth in human corneal epithelial cells. J Biol Chem 2005;280:32230-32237.

25 Yang H, Sun X, Wang Z, Ning G, Zhang F, Kong J, Lu L, Reinach PS: EGF stimulates growth by enhancing capacitative calcium entry in corneal epithelial cells. J Membr Biol 2003;194:47-58.

26 Panet R, Eliash M, Pick M, Atlan H: Na$^+$/K$^+$/Cl$^-$ cotransporter activates mitogen-activated protein kinase in fibroblasts and lymphocytes. J Cell Physiol 2002;190:227-237.

27 Flemmer AW, Gimenez I, Dowd BF, Darman RB, Forbush B: Activation of the Na-K-Cl cotransporter nkcc1 detected with a phospho-specific antibody. J Biol Chem 2002;277:37551-37558.

28 Xu KP, Dartt DA, Yu FS: EGF-induced erk phosphorylation independent of PKC isozymes in human corneal epithelial cells. Invest Ophthalmol Vis Sci 2002;43:3673-3679.

29 Brondello JM, Pouyssegur J, McKenzie FR: Reduced map kinase phosphatase-1 degradation after p42/p44MAPK-dependent phosphorylation. Science 1999;286:2514-2517.

30 Kucharska A, Rushworth LK, Staples C, Morrice NA, Keyse SM: Regulation of the inducible nuclear dual-specificity phosphatase DUSP5 by Erk MAPK. Cell Signal 2009;21:1794-1805.

31 Islam M, Akhtar RA: Upregulation of phospholipase cgamma1 activity during EGF-induced proliferation of corneal epithelial cells: Effect of phosphoinositide-3 kinase. Invest Ophthalmol Vis Sci 2001;42:1472-1478.

32 Kang SS, Li T, Xu D, Reinach PS, Lu L: Inhibitory effect of pge2 on EGF-induced map kinase activity and rabbit corneal epithelial proliferation. Invest Ophthalmol Vis Sci 2000;41:2164-2169.

33 Kang SS, Wang L, Kao WW, Reinach PS, Lu L: Control of sv-40 transformed rce cell proliferation by growth-factor-induced cell cycle progression. Curr Eye Res 2001;23:397-405.

34 Cai L, Du T, Song D, Li B, Hertz L, Peng L: Astrocyte erk phosphorylation precedes K$^+$-induced swelling but follows hypotonicity-induced swelling. Neuropathology 2011;31:250-264.

35 Hannemann A, Flatman PW: Phosphorylation and transport in the Na-K-2Cl cotransporters, nkcc1 and NKCC2a, compared in HEK-293 cells. PLoS One 2011;6:e17992.

36 Hodges RR, Horikawa Y, Rios JD, Shatos MA, Dartt DA: Effect of protein kinase C and Ca^{2+} on p42/p44 MAPK, PYK2, and SRC activation in rat conjunctival goblet cells. Exp Eye Res 2007;85:836-844.

37 Nurmi A, Goldsteins G, Narvainen J, Pihlaja R, Ahtoniemi T, Grohn O, Koistinaho J: Antioxidant pyrrolidine dithiocarbamate activates AKT-GSK signaling and is neuroprotective in neonatal hypoxia-ischemia. Free Radic Biol Med 2006;40:1776-1784.